2854 J. Med. Chem. 2010, 53, 2854–2864
DOI: 10.1021/jm9016812

Journal of Medicinal Chemistry Article

Discovery of an Oxybenzylglycine Based Peroxisome Proliferator Activated Receptor α Selective Agonist 2-((3-((2-(4-Chlorophenyl)-5-methyloxazol-4-yl)methoxy)benzyl)(methoxycarbonyl)-amino)acetic Acid (BMS-687453)

Jun Li,*,† Lawrence J. Kennedy,† Yan Shi,† Shiwei Tao,† Xiang-Yang Ye,† Stephanie Y. Chen,† Ying Wang,† Andrés S. Hernández,† Wei Wang,† Pratik V. Devasthale,† Sean Chen,† Zhi Lai,† Hao Zhang,† Shung Wu,† Rebecca A. Smirk,† Scott A. Bolton,† Denis E. Ryono,† Huiping Zhang,⊥ Ngiap-Kie Lim,⊥ Bang-Chi Chen,⊥ Kenneth T. Locke,§ Kevin M. O'Malley,§ Litao Zhang,§ Rai Ajit Srivastava,‡ Bowman Miao,‡ Daniel S. Meyers,‡ Hossain Monshizadegan,‡ Debra Search,‡ Denise Grimm,‡ Rongan Zhang,‡ Thomas Harrity,‡ Lori K. Kunselman,‡ Michael Cap,‡ Pathanjali Kadiyala,‡ Vinayak Hosagrahara,∥ Lisa Zhang,∥ Carrie Xu,∥ Yi-Xin Li,∥ Jodi K. Muckelbauer,# Chiehying Chang,# Yongmi An,∞ Stanley R. Krystek,× Michael A. Blanar,‡ Robert Zahler,† Ranjan Mukherjee,‡ Peter T. W. Cheng,† and Joseph A. Tino†

†*Metabolic Diseases Chemistry,* ‡*Metabolic Diseases/Atherosclerosis Biology,* §*Lead Evaluation,* ∥*Preclinical Candidate Optimization,* ⊥*Department of Chemical Synthesis,* #*Macromolecular Crystallography,* ∞*Gene Expression and Protein Biochemistry, and* ×*CADD, Bristol-Myers Squibb, Building 13, P.O. Box 5400, Princeton, New Jersey 08543-5400*

Received November 13, 2009

An 1,3-oxybenzylglycine based compound **2** (BMS-687453) was discovered to be a potent and selective peroxisome proliferator activated receptor (PPAR) α agonist, with an EC_{50} of 10 nM for human PPARα and ~410-fold selectivity vs human PPARγ in PPAR-GAL4 transactivation assays. Similar potencies and selectivity were also observed in the full length receptor co-transfection assays. Compound **2** has negligible cross-reactivity against a panel of human nuclear hormone receptors including PPARδ. Compound **2** demonstrated an excellent pharmacological and safety profile in preclinical studies and thus was chosen as a development candidate for the treatment of atherosclerosis and dyslipidemia. The X-ray cocrystal structures of the early lead compound **12** and compound **2** in complex with PPARα ligand binding domain (LBD) were determined. The role of the crystal structure of compound **12** with PPARα in the development of the SAR that ultimately resulted in the discovery of compound **2** is discussed.

Introduction

Atherosclerosis/cardiovascular disease is the leading cause of death for adults in developed countries. Among the predominant risk factors for atherosclerosis are high levels of low-density lipoprotein-cholesterol (LDLc[a]) and triglycerides and low levels of high-density lipoprotein-cholesterol (HDLc). Although considerable progress has been made in the discovery of therapeutics that lower LDLc (especially statins), atherosclerosis still remains a leading cause of mortality in the developed countries. Several clinical studies have indicated the limitations of the strategy of reducing atherosclerotic cardiovascular disease by lowering LDLc alone without treatment of other lipid risk factors.[1] Thus, there has been a gradual realization that additional risk factors beyond LDLc need to be targeted in order to address the very substantial residual risk of cardiovascular disease. HDLc levels have been found to be inversely correlated with the risk of coronary artery diseases (CAD). Several clinical trials have shown a marked decrease in the incidence of CAD with increased plasma HDLc.[2] Additionally, high triglyceride levels have also been correlated with increased cardiovascular risk.[3] Hence, a combination of intensive LDLc lowering along with HDLc elevation as well as reduction of triglyceride levels may greatly benefit the treatment of atherosclerosis in cornary disease patients.

The peroxisome proliferator activated receptor α (PPARα) is a member of the intracellular nuclear hormone receptor superfamily of transcription factors. Upon binding of ligand agonists, there is a conformational change that leads to the modulation of a number of PPARα responsive genes. These genes in turn have pleiotropic effects on plasma lipoprotein levels, atherosclerosis, insulin sensitization, and inflammation.[4] The endogenous ligands for PPARα are believed to be fatty acids, and synthetic ligands include the fibrate class of hypolipidemic drugs (fenofibrate, gemfibrozil, and bezafibrate) currently in clinical use.[4a,14] For the past several decades, the fibrates have been broadly utilized for the treatment of dyslipidemia and hypertriglyceridemia.[5] This class of drugs is also used as combination therapy for diabetics, and their new applications are continuously being explored.[6] Recently, a delayed-release formulation of fenofibrate for use along with diet has been shown to help in lowering triglycerides and LDLc, as well as raising HDLc in dyslipidemic patients. Clinical trials with this new formulation of fenofibrate have demonstrated that when used in combination with the most commonly prescribed statins, it has helped

*To whom correspondence should be addressed. Telephone: 609-818-7123. Fax: 609-818-6810. E-mail: jun.li@bms.com.

[a] Abbreviations: PPAR, peroxisome proliferator activated receptor; LBD, ligand binding domain; LDLc, low-density lipoprotein-cholesterol; HDLc, high-density lipoprotein-cholesterol.

 Published on Web 03/10/2010

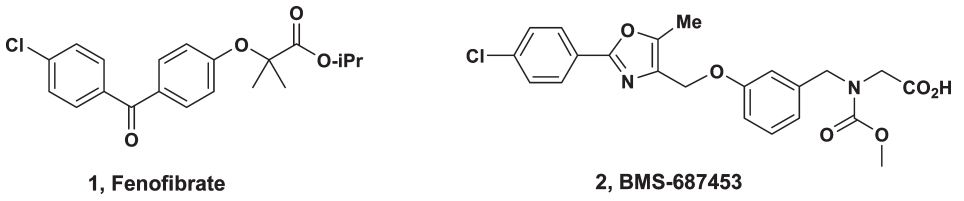

Figure 1. Small molecule PPARα agonists.

Scheme 1[a]

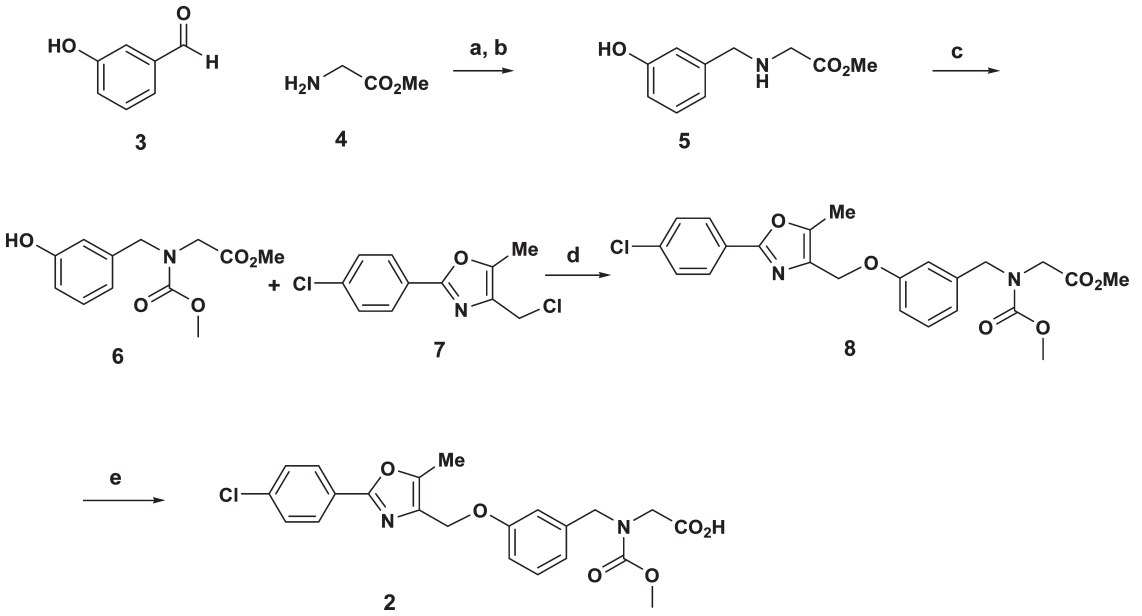

[a] Reagents and conditions: (a) Et_3N, MeOH, room temp; (b) $NaBH_4$, 0 °C to room temp, 95% for two steps; (c) methyl chloroformate, aq $NaHCO_3$, THF, 99%; (d) K_2CO_3, MeCN, 70 °C, 71%; (e) LiOH, THF, room temp, 93%.

patients manage all three key lipids better than the corresponding therapies alone.[7] Despite the general concern for the side effects and carcinogenetic potential of PPAR class drugs, in vitro and in vivo potential antitumor properties of fenofibrate and other PPARα agonists through direct and indirect antiangiogenic effects, as well as anti-inflammatory activity, have also been reported recently.[8] Those findings may further stimulate the study of the potential clinical benefits of fenofibrate or other PPARα agonists in cancer treatments, along or in combination with other therapies, or as a potential tumor-preventative agent, in addition to its antiatherosclerosis.

In spite of their use in clinical settings, the fibrate drugs are very weak affinity ligands for PPARα, which results in the relatively high doses (e.g., 200 mg of fenofibrate) needed to achieve clinical efficacy, and unwanted side effects may occur at these high doses. These dose-limiting side effects of the fibrates may be limiting their broader clinical usage, thus preventing maximal efficacy of these drugs in protecting against cardiovascular disease. In the past several years, several potent PPARα selective agonists have been progressed into various phases of clinical development.[9] However, the development of most of these potent and selective PPARα agonist clinical candidates has been suspended and none of them have reached the market because of various reasons including (primarily) safety concerns. A potent and efficacious PPARα agonist with an excellent safety profile may provide an opportunity for the treatment of atherosclerosis and dyslipidemia as well as further lowering the risk of CAD with minimized side effects. Herein we report the oxybenzylglycine based compound **2** (Figure 1) as a potent, highly selective PPARα agonist with an excellent preclinical safety profile.

Chemistry

The synthesis of compound **2** is described in Scheme 1. Reductive amination of 3-hydroxybenzaldehyde **3** with glycine methyl ester hydrochloride **4** afforded the secondary amine **5** as a colorless solid in 95% yield. Condensation of amine **5** with methyl chloroformate gave the methyl carbamate **6** in 99% yield as a light-yellow oil. Compound **6** was reacted with the chloromethyloxazole **7** in the presence of base at 80 °C to give the methyl ester **8** as a colorless solid in 71% yield after column chromatography. Hydrolysis of ester **8** with aqueous lithium hydroxide gave compound **2** as a colorless solid in 93% yield. The compounds **9**−**32** were synthesized in analogous fashion as described above.

Results and Discussion

During the course of our concurrent work on PPARα/γ dual agonists, we made the following observations in our transactivation assay (see Table 1).[10] Compound **9** (Figure 2), which has a two-carbon ethoxy linker between the 1, 4-oxybenzylglycine and phenyloxazole, is a relatively selective PPARγ agonist, whereas the corresponding analogue **10**, which has a one-carbon linker, is almost equipotent at

Table 1. In Vitro Transactivation EC_{50} and Binding IC_{50} Data of Early Leads[a]

compd	α-EC_{50} (nM)	γ-EC_{50} (nM)	γ/α EC_{50} ratio	α-IC_{50} (nM)	γ-IC_{50} (nM)	γ/α IC_{50} ratio
9	289.3	75.4	0.26	941.8	141.4	0.15
10	39.1	41.5	1.06	811.2	247.8	0.30
11	16.5	141.2	8.54	610.1	162.0	0.27
12	8.8	1321	150.0	347.0	2789.0	8.04

[a] Compounds were tested for agonist activity on hPPAR-GAL4 HEK transactivation assay. Full PPARα intrinsic activity (relative to fenofibric acid) was observed for all tested compounds.

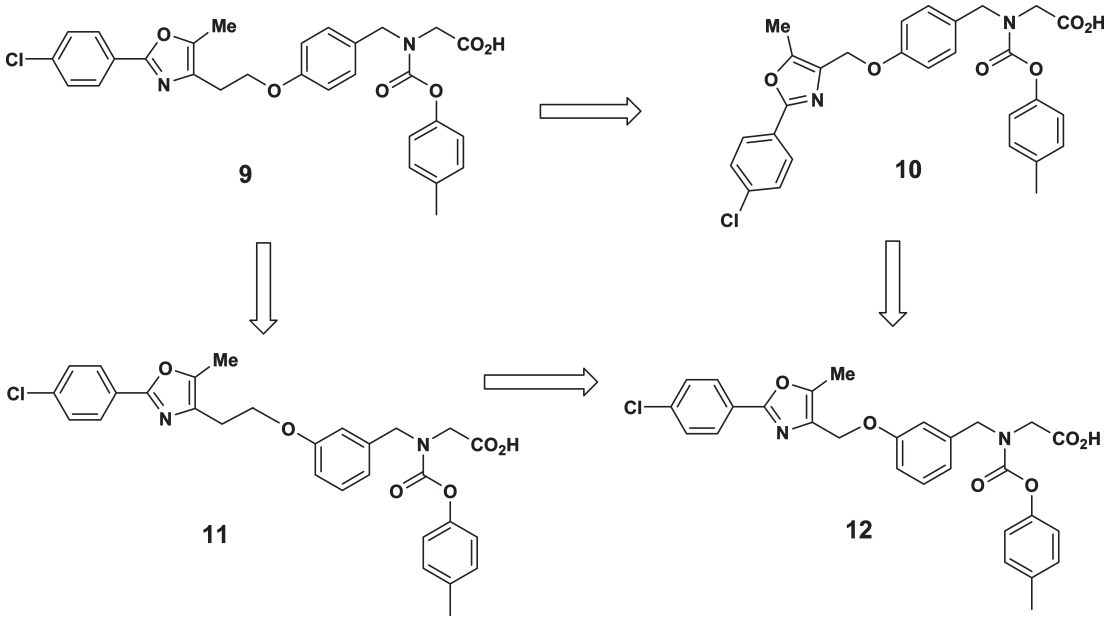

Figure 2. Early lead evolution.

PPARα and PPARγ. On the other hand, the closely related 1,3-oxybenzylglycine analogue **11** was an 8-fold selective PPARα agonist vs PPARγ. With this in mind, a hybrid compound **12**, which incorporated a one-carbon linker into the 1,3-oxybenzylglycine framework of **11**, was prepared. As anticipated, this compound was a highly potent PPARα agonist with >200-fold PPARα selectivity vs PPARγ. The binding affinity also gave a similar selectivity trend for these lead compounds. Although compound **12** fulfills our criteria for in vitro PPARα potency and selectivity vs PPARγ, it has significant issues that preclude it from further advancement, including ion channel activity (93% inhibition at 30 μM in hERG and 58% inhibition at 10 μM in sodium channel patch clamp assays, respectively) and CYP-450 inhibitory activity (e.g., IC_{50} = 1.2 μM for the CYP 2C-9 isozyme). Additionally, compound **12** only showed weak to moderate effects in standard in vivo efficacy models, e.g., failing to lower LDLc levels in high fat fed hamsters at doses up to 10 (mg/kg)/day in a 21-day study.

To attempt to understand the selectivity of **12**, an X-ray cocrystal structure of **12** with the PPARα ligand binding domain (LBD) was determined to 2.1 Å resolution (Figure 3).[11] Indeed, the 1, 3 oxybenzylglycine central core was found to fit well within the PPARα binding pocket. As expected, the well-recognized hydrogen-bonding network was observed between the carboxylic acid of **12** and neighboring residues (His 440, Tyr 464, Tyr 314, and Ser 280), which is believed to be critical for the functional activity of PPARα ligands. In addition to these standard carboxylate interactions with the binding pocket, an interesting indirect hydrogen bond was also observed between the oxazole nitrogen, water, and Thr 279. The remaining interactions between ligand and protein are hydrophobic in nature. In particular, the tolyl carbamate moiety was observed to bind into a hydrophobic pocket defined by Ile 272, Phe 273, Leu 347, Phe 351, Ile 354, and Met 355; no hydrogen bonds or ionic interactions with the surrounding residues existed. We believed that SAR investigations could be conducted within this portion of the molecule to further optimize compound binding affinity or reduce potential liabilities. Additionally, the function of the chloro substituent of the phenyl group was also unclear in this binding mode in the PPARα crystal structure, although it significantly increased the PPARα selectivity in our in vitro assay. For example, compound **18** (see Table 3), a close analogue of **12** with a hydrogen rather than Cl at the para-position, lost almost 6-fold in PPARα potency.

With lead compound **12** in hand, we initiated a systematic SAR study that targeted each of its separate putative pharmacophores. The transactivation assay (EC_{50}) was employed as our primary assay for SAR studies because of its better correlation with the in vivo efficacy in our hands. Our first approach focused on the left-hand portions of the molecule. To test the indirect hydrogen-bond interaction between the oxazole nitrogen with the PPARα binding pocket as shown in Figure 3, three close analogues of **12** were prepared (Table 2). Interestingly, the differences in binding affinities between these compounds were smaller than we expected. However, the results from the functional assay did indicate that the regiochemical orientation of the original oxazole of **12** is very important/optimal. For example, compound **13** (where the

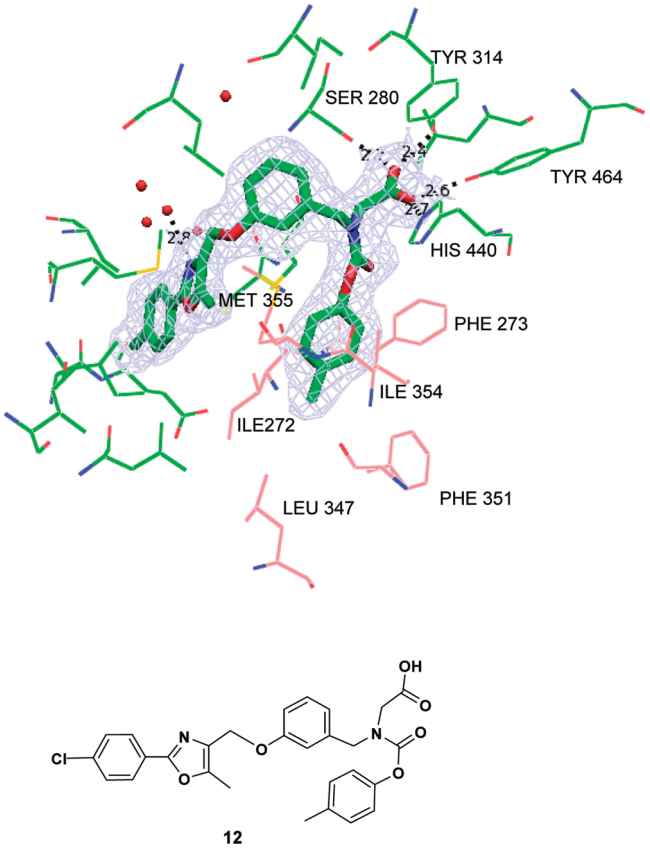

Figure 3. The X-ray crystal structure of PPARα LBD with compound **12** is illustrated at 2.1 Å resolution. Compound **12** is shown as thick sticks and also as a 2D representation. Protein side chains within 3.9 Å of the compound are shown as thin sticks. Residues of the hydrophobic pocket surrounding the tolyl group are shown with orange carbons. $2F_o - F_c$ electron density is shown as light-blue mesh contoured at 1σ around the compound. Water molecules are shown as red spheres. Hydrogen bonds are shown as black dashed lines. PDB deposition number for PPARα and compound **12** is 3KDU.

oxazole 4- and 5-substituents are reversed relative to **12**) was significantly less active than **12** in the PPARα functional assay and had significantly reduced PPARα selectivity vs PPARγ. In addition, compounds **14** and **15**, where a larger thiazole and "reversed" thiazole respectively replace the original oxazole of **12**, exhibited similarly attenuated PPARα binding affinity. Unlike their corresponding oxazole analogues, the two thiazole analogues **14** and **15** also showed similar potency in the functional PPARα assay. All these results suggested that the indirect hydrogen-bond interaction in this portion of the molecule might not be critical for optimal binding affinity. However, our SAR study at this portion of the molecule indicated that the oxazole moiety with the substitution pattern of **12** is optimal and plays a critical role in maintaining the potent PPARα functional activity.

Our next approach focused on the "left hand" portion of the molecule, the phenyloxazole moiety, with the initial focus being the effects of the phenyl ring substituents on PPARα/γ activity. The results are shown in Table 3. Moving the *p*-chloro group of **12** to the ortho and meta positions (**16**, **17**) reduced both PPARα potency (EC_{50}) and selectivity, suggesting that the para-position may be optimal for further SAR studies to optimize the phenyl substituent(s). A small substituent such as fluorine (**19**) at the para-position slightly attenuated the PPARα but maintained the PPARγ transactivation activity. Interestingly, a bulky aliphatic substituent such as *tert*-butyl significantly improved the PPARγ potency while maintaining PPARα potency. This modification resulted in a very potent and well balanced PPARα/γ agonist **20** (EC_{50} ratio $\gamma/\alpha = 2$). On the other hand, a 4-phenyl substituent only slightly improved PPARγ potency but considerably reduced PPARα functional potency, also resulting in a balanced PPARα/γ agonist **21** (EC_{50} ratio $\gamma/\alpha = 1.2$) but with relatively weak overall functional potency. Unexpectedly, a saturated, polar six-membered analogue with N-linked morpholine (**22**) slightly improved functional potency and selectivity compared to the aromatic phenyl-substituted analogue **21**. These results prompted us to further examine the effect of varying the electronegativity of the substituent at the 4-phenyl position. A polar and electron withdrawing group (CN) at this position provided compound **23** with good PPARα potency with 93-fold PPARα selectivity vs PPARγ in the transactivation assay. Interestingly, an electron-donating substituent such as methoxy gave a compound **24** with similar functional potency and selectivity to **23**, although their binding affinities are significantly different. This result indicated that the electronic effect of the substituents on the phenyl ring had minimal consequences on functional potency or selectivity but may play a more influential role in binding affinity. Steric effects may play a more dominant role in determining PPARγ functional activity in this portion of the molecule. For example, two comparably sized substituents that have different electronic properties, isopropyl (**26**) and trifluoromethyl (**27**) at the para position of the phenyl, afforded analogues with very similar functional potencies and selectivities. On the other hand, analogues with a small methyl group (**25**) and a bulky *tert*-butyl group (**20**) have very different PPARγ functional potencies, thus resulting in a significant disparity in selectivity, although they have similar PPARα potency. The SAR trend of the binding affinity is not clear for this portion of the molecule. Overall, the SAR study of this part of the molecule has indicated that the 4-Cl-phenyl moiety was optimal, providing the highest level of PPARα potency and selectivity. Additionally, none of the phenyl-substituted analogues with acceptable potency or selectivity showed any significant improvement in comparison with the lead compound **12** with respect to CYP 2C9 inhibition or electrophysiological hERG activity (Table 4).

Focusing on eliminating both the cardiovascular liabilities and the CYP inhibitory activities of the lead molecule **12**, we then turned our attention to modify its other pharmacophores. As indicated in the analysis of the X-ray structure of **12**, although the tolyl carbamate group of the "right-hand" portion of the molecule fits well into a hydrophobic pocket defined by residues Ile 272, Phe 273, Leu 347, Phe 351, Ile 354, and Met 355, we hypothesized that alternative/additional functionalities could be explored and may be tolerated in this region. To test this hypothesis, we first examined the cyclohexyl carbamate analogue **28**, which is the aliphatic counterpart of compound **12**. As anticipated, compound **28** possessed similar PPARα potency and excellent selectivity. Systematically reducing the cycloalkyl ring size from six to three resulted in compounds **29**−**31**, all of which provided excellent PPARα potency and good to excellent selectivity. We then extended this portion of the SAR study to noncyclic alkyl carbamates. This effort revealed that small, noncyclic alkyl carbamates provided even better PPARα selectivity. For example, compound **32**, an *n*-propyl carbamate, achieved >200-fold

Table 2. In Vitro Activity of Alternative Heterocyclic Analogues[a]

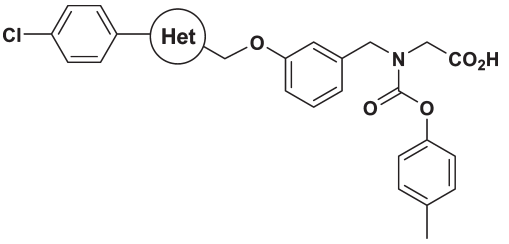

Compound	Het	αEC50 (nM)	γEC50 (nM)	γ/α EC50 Ratio	α–IC50 (nM)	γ–EC50 (nM)	γ/α IC50 Ratio
13	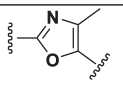	122	2901	24	485	3546	7.3
14	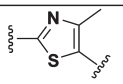	101	1411	14	708	4057	5.7
15	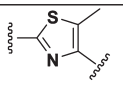	90	2500	28	582	3362	5.7

[a] Compounds were tested for agonist activity in the hPPAR-GAL4 HEK transactivation assays. Full PPARα intrinsic activity (relative to fenofibric acid) was observed for all tested compounds. $n = 1-3$.

Table 3. In Vitro Activity of Substituted Phenyloxazole Analogues[a]

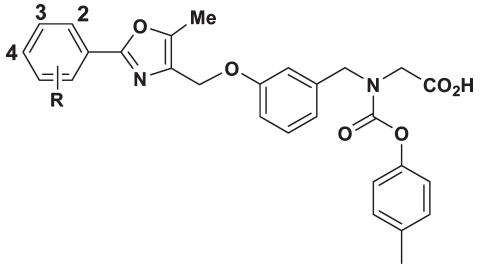

compd	R	α-EC50 (nM)	γ-EC50 (nM)	γ/α EC50 ratio	α-IC50 (nM)	γ-IC50 (nM)	γ/α IC50 ratio
12	4-Cl	8.8	1321	150	347	2789	8.0
16	2-Cl	68.0	1100	16	420	1039	2.5
17	3-Cl	134	520	3.9	422	384	0.9
18	4-H	48.6	705	15	NA	NA	NA
19	4-F	20.5	1007	49	362	2300	6.3
20	4-C$(CH_3)_3$	10.0	20.1	2	1324	483	0.36
21	4-Ph	340	398	1.2	2885	1988	0.69
22	4-morpholine	108	417	3.9	1725	1194	0.69
23	4-CN	37.0	3445	93	473	7257	15.3
24	4-MeO	15.8	1124	71	375	873	2.3
25	4-Me	9.1	684	75	372	1361	3.6
26	4-C$H(Me)_2$	8.7	284	32	526	497	0.94
27	4-CF_3	12.0	705	59	569	2737	4.8

[a] Compounds were tested for agonist activity in the hPPAR-GAL4 HEK transactivation assays. Full PPARα intrinsic activity (relative to fenofibric acid) was observed for all tested compounds. $n = 1-3$.

α/γ selectivity. Following up on this SAR trend, further reducing the carbamate size led to the discovery of lead compound **2**, a methyl carbamate with excellent PPARα potency and 410-fold PPARα/γ selectivity.

Table 4. CYP 2C-9 Isozyme Inhibition and hERG Inhibition IC_{50}

parameter	**12**	**13**	**14**	**15**	**16**	**17**	**19**	**23**	**24**	**25**	**27**
CYP 2C9 IC_{50} (μM)	1.2	3.4	3.7	7.1	3.7	0.5	8.6	21	2.8	3.5	4.4
hERG flux IC_{50} (μM)	29.3	20.0	> 80	10.0	> 80	7.3	38	53.0	8.6	25.9	26

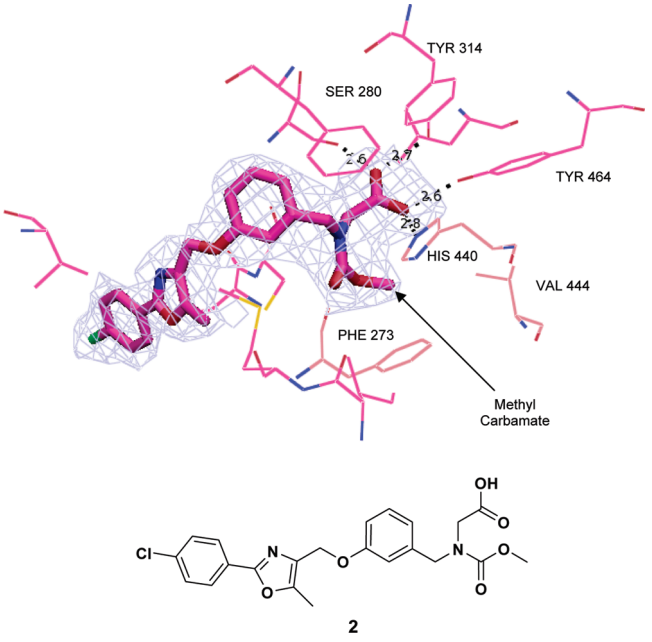

Figure 4. X-ray crystal structures of PPARα LBD to 2.7 Å resolution confirming the binding mode of compound **2**. Protein side chains within 4 Å of compound are shown as thin sticks. Residues surrounding the carbon atom of the methyl carbamate are shown with orange carbons. All other carbons are shown in purple. Compound is shown as thick sticks and also as a 2D representation. $2F_o - F_c$ electron density is shown as light-blue mesh contoured at 1σ around the compound. Hydrogen bonds are shown as black dashed lines. PDB deposition number for PPARα and compound **2** is 3KDT.

The X-ray crystal structure of compound **2** bound to PPARα was determined to 2.7 Å resolution (Figure 4).[11] The structure confirmed the anticipated binding mode of compound **2** and revealed very similar binding conformations between compounds **12** and **2** to PPARα. As observed for the X-ray structure of compound **12**, the same hydrogen bonding network is observed between the carboxylic acid and residues Tyr 464, His 440, Tyr 314, and Ser 280. Interestingly, the ether oxygen of the carbamate of compound **2** flips in orientation relative to compound **12**, leaving the methyl group extended toward Phe 273, His 440, and Val 444, and the oxygen extended toward the now empty hydrophobic pocket.

The potency and selectivity of compound **2** were further confirmed by testing it in co-transfection assays in HepG2 cells using full length human PPARα and PPARγ. In this assay, compound **2** showed excellent PPARα potency (EC_{50} = 47 nM) with ~50-fold selectivity vs PPARγ (EC_{50} = 2400 nM). This result correlated well with the data observed from the primary GAL-4 HEK transactivation based screening assays as shown in Table 5. Compound **2** was found to be less potent in rodent PPARα functional assays, with a moderate EC_{50} of 426 nM for mouse and 488 nM for hamster but remains a full PPARα agonist in both species.[12] Importantly, compound **2** showed negligible activity (EC_{50} for transactivation of > 25 μM and efficacies of < 15% of standard) against a panel of human nuclear hormone receptors, including PPARδ LXR and RXR.

A human ApoA1 transgenic mouse model was employed to evaluate the impact of compound **2** on serum HDLc and triglyceride levels. PPARα agonists such as fibrates lower triglycerides and raise HDLc levels in humans. One of the pathways by which this is accomplished is by increasing ApoA1, the main protein component of the HDL particle. However, in normal mice, the murine promoter causes a reduction (rather than an increase, as in humans) in apoA1 and thereby reduces HDL levels.[18a] Therefore, transgenic mice overexpressing human ApoA1 under the control of the natural human (rather than the murine) ApoA1 promoter are widely used to evaluate the HDLc elevating properties of PPARα agonists.[18b] Compound **2** and fenofibrate were thus evaluated in the human ApoA1 transgenic mouse model in a 10-day dose response study. These mice still express mouse PPARα, and compound **2** in the GAL4-mouse PPARα assay has an EC_{50} value of 426 nM, which is 43-fold less than its activity at human PPARα. Therefore, the use of high doses of compound **2** would be expected to be needed to demonstrate efficacy. As shown in Table 6, serum ApoA1 protein levels after 10 days of treatment of compound **2** were increased in a dose-dependent manner, with the maximal effect likely seen at the 50−100 (mg/kg)/day dose. These data corroborate the HDLc elevations observed at these doses (Table 6). As a reference, fenofibrate at the 100 (mg/kg)/day dose raised HDLc by 62% after 10 days. By comparison, compound **2**, after 10 days of treatment, also showed dose-dependent increases in serum HDLc and reductions in triglycerides. The maximal effect (plateau) was achieved at the 50 (mg/kg)/day dose where the elevation of HDLc was 135% and the triglyceride lowering was 78%. These data clearly demonstrated that compound **2** can robustly elevate HDLc and lower triglycerides in the human ApoA1 transgenic mouse model.

The high fat fed hamster was another animal model used to further evaluate the in vivo efficacy of compound **2**. Hamsters are very responsive to a high fat diet; the fasting triglyceride levels and plasma total cholesterol levels (mainly LDLc) are elevated following the high fat feeding, but HDLc levels remain relatively unchanged. The advantage of the hamster model is that the level of hepatic cholesterol synthesis in hamsters is similar to that in humans, and the serum lipid profile of high fat diet-fed hamsters resembles that of dyslipidemic humans with pronounced LDL and VLDL cholesterol peaks.[19] The hamster has been shown to be a useful preclinical model of human lipoprotein metabolism and atherosclerosis.[20] In our study, the hamster model was primarily used for evaluation of the compound's efficacy to lower triglyceride and LDLc levels.

Evaluation of the efficacy of compound **2** was conducted in a dose response study ranging from 1 to 10 (mg/kg)/day for 3 weeks. Table 7 shows the fasting plasma lipid parameters at the conclusion of the study. Compound **2** lowered plasma triglycerides by 60% at the 3 (mg/kg)/day dose and 91% at the 10 (mg/kg)/day dose, suggesting that the effect of compound **2** on triglycerides lowering reaches a plateau at the 10 (mg/kg/)

Table 5. In Vitro Activity of Aliphatic Carbamate Analogues[a]

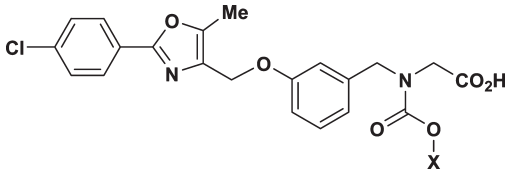

compd	X	α-EC_{50} (nM)	γ-EC_{50} (nM)	γ/α EC_{50} ratio	α-IC_{50} (nM)	γ-IC_{50} (nM)	γ/α IC_{50} ratio
28	cyclohexyl-	7.5	843	112	513	4498	8.8
29	cyclopentyl-	9.2	1482	161	408	9444	23.1
30	cyclobutyl-	12.5	905	72	228	5293	23.2
31	cyclopropylmethyl-	6.3	826	131	351	5336	15.2
32	*n*-propyl-	6.0	1257	209	336	10310	30.7
2	Me-	10	4100	410	260	>15000	>57

[a] Compounds were tested for agonist activity on hPPAR-GAL4 HEK transactivation assay. Full PPARα intrinsic activity (relative to fenofibric acid) was observed for all tested compounds. $n = 1-3$.

Table 6. Effect of Compound **2** and Fenofibrate on Plasma Parameters in Human ApoA1 Transgenic Mice[a]

treatment	serum hu-ApoA1 mg/dL ± SEM (% change)	TG mg/dL ± SEM (% change)	HDLc mg/dL ± SEM (% change)
vehicle	693 ± 51	189 ± 32.9	158 ± 18.5
fenofibrate, 100 (mg/kg)/day	1957 ± 138 (182%*)	64.1 ± 3.0 (−66%*)	255 ± 21.3 (61.7%*)
compound **2**, 10 (mg/kg)/day	1163 ± 61 (67.88%*)	95.8 ± 3.7 (−49.4%*)	250 ± 29.6 (58.1%*)
compound **2**, 50 (mg/kg)/day	2219 ± 176 (220%*)	72.6 ± 7.1 (−61.7%*)	372 ± 20.5 (135.4%*)
compound **2**, 100 (mg/kg)/day	2511 ± 158 (262%*)	40.8 ± 3.2 (−78.5%*)	364 ± 27.1 (130.1%*)

[a] $p < 0.05$ compared to vehicle-treated group ($n = 10$). ApoA-I transgenic mice ($n = 10$) were treated for 10 days with compound dosed by oral gavage. Blood was drawn after a 4 h fast on day 10 after the final dose to measure plasma lipids. Human ApoA1 protein in the serum was measured by a using apolipoprotein A1 kit (Polymedco). Also see ref 12.

Table 7. Effect of Compound **2** on Plasma Parameters in High Fat-Fed Hamsters[a]

entry	vehicle	fenofibrate (100 mg/kg)	compound **2** (1 mg/kg)	compound **2** (3 mg/kg)	compound **2** (10 mg/kg)
TG mg/dL ± SEM (% change)	644 ± 139	132 ± 20 (−79%)	784 ± 195 (+21%)	258 ± 51 (−60%)	58 ± 5 (−91%)
LDLc mg/dL ± SEM (% change)	326 ± 53	93 ± 12 (−71%)	196 ± 21 (−40%)	97 ± 10 (−70%)	42 ± 4 (−87%)

[a] $p < 0.05$ versus vehicle control. Compound **2** lower serum triglycerides and LDLc in fat fed hamsters. Male Syrian golden hamsters on a high fat diet were dosed daily by oral gavage for 21 days. Blood samples were drawn for serum lipid measurements after an 18 h fast and 24 h after the last dose. Fenofibrate (Feno) at 100 mpk was used as a positive control. The compounds and doses are indicated. Data represent the mean ± SEM ($n = 8$). Also see ref 12.

Table 8. Pharmacokinetic Profile of **2**[a]

species	dose route	dose (mg/ kg)	T_{max} (h)	C_{max} (μM)	AUC (μM·h)	CL_{PI} ((mL/min)/kg)	V_{ss} (L/kg)	$T_{1/2}$ (h)	*F* (%)
mouse	iv	6			19.3[b]	10.8	1.3	3.0	
	po	12	0.25	23.8	33.9[b]				88
rat	ia[c]	5			48 ± 9	4.3 ± 0.9	0.7 ± 0.1	3.2 ± 0.2	
	po	10	0.4 ± 0.1	43 ± 14	88 ± 10				91
dog	iv	1			3.9 ± 0.3	9.5 ± 0.7	1.8 ± 0.8	7.9 ± 4.1	
	po	2	0.9 ± 0.1	1.0 ± 0.6	4.5 ± 2.0				58
monkey	iv	1			5.8 ± 3.6	8.9 ± 4.1	3.5 ± 1.7	11.9 ± 4.0	
	po	2	0.8 ± 0.3	1.9 ± 0.7	8.5 ± 4.9				75

[a] For each experimental study, $n \geq 3$. [b] AUC_{0-8h} reported here, not AUC_{INF}. [c] Intra-arterial administration.

day dose. Similar effects were also observed on LDLc with 70% and 87% reductions at the 3 and 10 (mg/kg)/day doses, respectively. Overall, compound **2** significantly lowers plasma triglycerides and LDLc in the chronic dyslipidemic hamster model.

As shown in Table 8, compound **2** has an excellent pharmacokinetic profile across all tested animal species. The oral absorption was rapid, with T_{max} ranging between 0.25 and 0.9 h in mouse, rat, dog, and cynomulgus monkey. The corresponding C_{max} values were 23.8 μM in mouse (12 mg/kg oral dose), 43 μM in rat (10 mg/kg oral dose), 1 μM in dog (2 mg/kg oral dose), and 1.9 μM/mL in monkeys (2 mg/kg oral dose). Compound **2** exhibited low plasma clearance in the mouse, rat, and monkey and moderate plasma clearance in the dog, and the volume of distribution ranged from 0.7 L/kg (rat) to 3.5 L/kg (cynomolgus monkey), which was comparable to the total body water in the rat and greater than total body water in the mouse, dog, and monkey. The half-life of compound **2** ranged from 3 h in mouse to 12 h in cynomolgus monkeys. Compound **2** also possessed excellent absolute oral

bioavailability ranging from 58% (dog) to 91% (rat). Additionally, compound **2** has excellent pharmaceutical properties, with a crystalline aqueous solubility being 280 μg/mL at pH 6.5, increasing to >4 mg/mL at pH 7.9.

Compound **2** was not a significant inhibitor of human CYP1A2, CYP2C8, CYP2C9, CYP2C19, CYP2D6, or CYP3A4 (IC_{50} > 40 μM). In addition, no induction of human PXR was observed up to 50 μM. No glutathione conjugates were detected when compound **2** at 30 μM was incubated with mouse, rat, or human liver microsomes fortified with glutathione (GHS, 5 mM). This result suggests that the overall formation of oxidative reactive metabolites may be low in humans in vivo. No in vitro liabilities were noted in extensive screens for receptor/enzyme binding inhibition, human hepatocyte toxicity, bacterial mutagenicity, or CHO cell clastogenicity. In comparison to lead compound **12**, compound **2** has a significantly improved cardiac ion channel liability profile. Compound **2** showed minimal activity against both hERG (1.8% at 10 μM and 4.0% at 30 μM in a patch-clamp assay) and sodium channels (at 10 μM drug, 6.9% inhibition at 1 Hz and 9.5% at 4 Hz). Additionally, no drug-related changes in cardiovascular parameters [e.g., hemodynamic and electrocardiographic (ECG) effects] were observed at up to 20 mg/kg compound **2** in a single-dose monkey telemetry study. Ames testing also showed that compound **2** was not mutagenic to the tester strains TA 98 and TA 100 at up to 5000 μg per plate.

In summary, compound **2** is a potent, orally active PPARα selective agonist that is highly efficacious in elevating HDLc in human ApoA1 transgenic mice and lowering LDLc in dyslipidemic hamsters in chronic studies. Compound **2** also robustly lowers plasma triglycerides in both animal models. The likelihood of drug−drug interaction of compound **2** should be minimal because of its negligible inhibition in all tested CYP isozymes or induction in the human PXR transactivation assay. No cardiovascular pharmacology safety issues were identified with in vitro screens as well as in preclinical animal models. On the basis of its excellent pharmacokinetic and pharmcodynamic properties, as well as superior in vitro liability profile, compound **2** was selected as a development candidate for further evaluation for the treatment of atherosclerosis.

Experimental Section

General Chemistry Methods. ^{1}H (400 MHz) and ^{13}C (100 MHz) NMR spectra were recorded on a JEOL GSX400 spectrometer using Me_4Si as an internal standard unless otherwise noted. LC−MS spectra were obtained on a Shimadzu HPLC and Micromass Platform using electrospray ionization. HRMS spectra were obtained on a Micromass LCT in lockspray with electrospray ionization. Analytical HPLC analyses were performed on a Shimadzu instrument using one of the following reverse phase methods, with UV detection set at 220 nm: (method A) Phenomenex S5 ODS 4.6 mm × 50 mm column, gradient elution 0−100% B/A over 4 min (solvent A = 10% MeOH/H_2O containing 0.1% H_3PO_4, solvent B = 90% MeOH/H_2O containing 0.1% H_3PO_4), flow rate 4 mL/min; (method B) Zorbax S5 SB-C18 4.6 mm × 75 mm column, gradient elution 0−100% B/A over 8 min (solvent A = 10% MeOH/H_2O containing 0.1% H_3PO_4, solvent B = 90% MeOH/H_2O containing 0.1% H_3PO_4), flow rate 2.5 mL/min. The purity of all final compounds is ≥95%, determined by analytic HPLC method A and confirmed by analytic HPLC method B.

Preparative HPLC was carried out on an automated Shimadzu system using YMC ODS C18 5 μm preparative columns with mixtures of solvent C (10% MeOH/90% H_2O/0.1% TFA) and solvent D (90% MeOH/10% H_2O/0.1% TFA) or of solvent E (10% CH_3CN/90% H_2O/0.1% TFA) and solvent F (90% CH_3CN /10% H_2O/0.1% TFA). All other reagents and solvents were obtained from commercial sources and were used without further purification.

Methyl 2-(3-Hydroxybenzylamino)acetate (5). To a solution of glycine methyl ester hydrochloride **4** (84.86 g, 0.67 mol) in MeOH (900 mL) was added Et_3N (68.29 g, 0.675 mol). After 15 min, a solution of 3-hydroxybenzaldehyde (75 g, 0.614 mol) in MeOH (500 mL) was added. After being stirred for 1 h, the reaction mixture was cooled to 0 °C, and $NaBH_4$ (5.7 g, 150 mmol) was then added portionwise over 20 min. After the mixture was stirred for 1 h, volatiles were removed in vacuo at 45−50 °C from the reaction mass. The resulting residue was partitioned between EtOAc (500 mL) and water (500 mL), with the aqueous layer being washed again with EtOAc(200 mL). The combined organic extracts were washed with brine, dried (Na_2SO_4), then concentrated in vacuo to afford the desired product **5** as a pale-yellow solid (113.9 g, 95%), which was used in the next step without further purification. ^{1}H NMR ($CDCl_3$, 400 MHz) δ 7.19 (t, J = 7.9 Hz, 1H), 6.87 (m, 1H), 6.81 (m, 1H), 6.72 (m, 1H), 3.76 (s, 2H), 3.74 (s, 2H), 3.43 (s, 3H); ^{1}H NMR (DMSO-d_6, 400 MHz) δ 9.26 (s, 1H), 7.07 (t, J = 8 Hz, 1H), 6.72 (s, 1H), 6.69 (d, J = 8 Hz, 1H), 6.61 (d, J = 1 Hz, 1H), 3.76 (s, 2H), 3.61 (s, 3H), 3.28 (s, 2H), 2.35 (s, 1H); ^{13}C NMR (DMSO-d_6, 100 MHz) δ 172.6, 157.4, 141.7, 129.9, 118.6, 114.8, 113.7, 52.1, 51.3, 49.3. LCMS $[M + H]^+$: 196.1.

Methyl 2-((3-Hydroxybenzyl)(methoxycarbonyl)amino)-acetate (6). To a stirred 0 °C solution of compound **5** (65.0 g, 333 mmol) in THF (325 mL) and saturated aqueous $NaHCO_3$ (260 mL) was added dropwise methyl chloroformate (25.7 mL, 333 mmol) over 20 min under nitrogen. The mixture was stirred at 0 °C for 45 min and extracted with EtOAc (2 × 260 mL). The organic extracts were dried over anhydrous Na_2SO_4, filtered, and concentrated in vacuo to give crude product **6** (83.8 g, 99.4%) as a yellow oil. The material was used directly in the next step without further purification. ^{1}H NMR ($CDCl_3$, 400 MHz) δ 7.19 (m, 1H), 6.78 (m, 3H), 6.14 (br s, 1H), 4.56 (s, 1H), 4.52 (s, 1H), 3.98 (s, 1H), 3.90 (s, 1H), 3.83 (s, 1.5H), 3.77 (s, 1.5H), 3.74 (s, 1.5H), 3.72 (s, 1.5H). ^{13}C NMR ($CDCl_3$, 100 MHz) δ170.2, 170.1, 157.4, 157.2, 156.6, 138.3, 138.2, 129.9, 129.8, 120.1, 119.4, 115.0, 114.8, 114.3, 53.3, 52.2, 51.4, 51.0, 47.8, 47.3. LCMS $[M + H]^+$: 254.2.

Methyl 2-((3-((2-(4-Chlorophenyl)-5-methyloxazol-4-yl)methoxy)-benzyl)(methoxycarbonyl)amino)acetate (8). To a solution of compound **6** (83.8 g, 331 mmol) in MeCN (700 mL) was added oxazole chloride **7** (80.1 g, 331 mmol) and anhydrous K_2CO_3 (137 g, 993 mmol). The mixture was heated at 70 °C for 21 h under nitrogen, cooled to 5 °C, poured into saturated aqueous NH_4Cl (1000 mL), and extracted with EtOAc (400 mL). The organic layer was dried over anhydrous Na_2SO_4, filtered, and concentrated in vacuo to yield the product (155.8 g) as a yellow syrup, which was purified by flash column chromatography (2.5 kg silica gel, elution with 20−50% EtOAc/heptane) to give the desired product **8** (108.1 g, 70.7%) as a colorless solid. Mp 83.4 °C. ^{1}H NMR ($CDCl_3$, 400 MHz) δ 7.97 (m, 2H), 7.42 (d, 2H, J = 8.4 Hz), 7.28 (m, 1H), 6.89 (m, 3H), 4.98 (s, 2H), 4.59 (s, 1H), 4.53 (s, 1H), 3.97 (s, 1H), 3.88 (s, 1H), 3.80 (s, 1.5H), 3.72 (s, 1.5H), 3.73 (s, 1.5H), 3.72 (s, 1.5H), 2.45 (s, 3H); ^{13}C NMR ($CDCl_3$, 100 MHz) δ170.5, 170.4, 159.5, 159.3, 159.2, 157.5, 157.3, 147.8, 138.9, 136.6, 136.6, 132.5, 130.2, 130.1, 129.4, 127.8, 126.3, 126.3, 121.4, 120.7, 114.9, 114.6, 114.3, 114.1, 62.5, 53.6, 52.5, 51.7, 51.4, 48.1, 47.6, 10.9; HRMS m/e 459.1323 (M^+). Anal. Calcd for $C_{23}H_{23}ClN_2O_6$: C, 60.20; H, 5.05; N, 6.10. Found: C, 60.41; H, 5.08; N, 6.00.

2-((3-((2-(4-Chlorophenyl)-5-methyloxazol-4-yl)methoxy)benzyl)-(methoxycarbonyl)amino)acetic Acid (2). To a stirred solution of methyl ester **8** (108 g, 235 mmol) in THF (732 mL) and water (366 mL) was added $LiOH \cdot H_2O$ (24.6 g, 585.9 mmol). The mixture was stirred at room temperature under nitrogen for 2 h and diluted with EtOAc (200 mL). The solution was brought to

pH 2 by the addition of aqueous 1 N HCl. The organic layer was separated, and the aqueous layer was extracted with EtOAc (2 × 250 mL). The combined organic extracts were washed with water (2 × 150 mL), dried over anhydrous Na_2SO_4, and concentrated in vacuo to give crude **2** (97 g, 93%). HPLC analysis showed that the purity of this batch was 98.5%.

For recrystallization, crude compound **2** (210 g, material combined from several batches) was dissolved in hot EtOAc (1200 mL) at 78 °C, then was cooled to room temperature over 60 min, then further cooled to 5 °C. The slurry was stirred at 5 °C for 40 min and filtered. The filter cake was washed with cold EtOAc (2 × 100 mL). The colorless solid was dried under vacuum at 55 °C for 8 h until a constant weight was obtained. The weight of the solid was 191 g (91% recovered yield). HPLC analysis showed that the purity of this batch was >99%. ^{1}H NMR (DMSO-d_6, 500 MHz, 65 °C) δ 12.47 (s, 1H), 7.93 (d, J = 8.8 Hz, 2H), 7.56 (d, J = 8.4 Hz, 2H), 7.25 (t, J = 8.1 Hz, 1H), 6.91−6.98 (m, 2H), 6.86 (d, J = 7.5 Hz, 1H), 4.98 (s, 2H), 4.44 (s, 2H), 3.85 (s, 2H), 3.62 (s, 3H), 2.43 (s, 3H). ^{13}C NMR (DMSO-d_6, 126 MHz, 19.8 °C) δ 170.7,170.6, 158.2, 157.9, 156.4, 147.8, 139.2, 135.0, 132.1, 129.2, 127.3, 125.6, 120.1, 119.7, 114.0, 113.4, 61.1, 52.6, 51.0, 50.6, 48.4, 47.9, 39.5, 9.9. HRMS-$(M + H)^+$ = 445.1173 (Δ = 1.4 ppm). Anal. Calcd for $C_{22}H_{21}ClN_2O_6$: C, 59.39; H, 4.75; N, 6.29; Cl, 7.97. Found: C, 59.40; H, 4.74; N, 6.22; Cl, 8.03.

Crystallography. Protein Expression and Purification. PPARα LBD (E196-Y468) protein was expressed and purified as described by Cronet et al.[21] with the following modifications. Freshly transformed *E. coli* (BL21-DE3, Novagen) were grown at 37 °C to an OD_{600nm} of 0.6 in M9 minimal media supplemented with casamino acids (Difco), trace minerals, and 30 μg/mL kanamycin. Cultures were chilled on ice for 30 min. Then overexpression was induced by addition of 0.4 mM isopropyl-β-D-thiogalactopyranoside, and the cultures were incubated for 18 h at 20 °C. Harvested cells were disrupted using a high-pressure homogenizer (Rannie). Supernatant loaded onto Ni-NTA was eluted with a 0−500 mM imidazole gradient. The histidine tag was removed using 10 units of human α-thrombin (Enzyme Research Labs) per 1.0 mg of purified protein for 2 h. At the completion of the cleavage reaction, thrombin was removed using a benzamidine resin. After removal of the histidine tag, PPARα was further polished on Q-Sepharose HP column (Amersham-Pharmacia Biotech) and protein elution was carried out with 10 column volumes of 20−500 mM NaCl gradient. The final samples were flash-frozen at 1.0 mg/mL concentration and stored at −80 °C.

Protein Crystallization. PPARα protein at 1.0 mg/mL in 20 mM Tris-HCl, pH 8.0, 0.15 M sodium chloride, 1 mM TCEP, and 10% glycerol was used for the crystallization trials with compounds **2** and **12**. Deoxy Big CHAP (DBC) was added to a final concentration of 0.7 mM before the addition of 5-fold molar excess compound to the protein solution. The complex was incubated at 4 °C overnight, concentrated to 8.0 mg/mL, and then diluted to 2.0 mg/mL with water just prior to crystallization. Crystal trials were performed at room temperature using the hanging-drop vapor-diffusion method. The hanging drop contained 1 μL of protein solution and 1 μL of reservoir solution (26−27% PEG 4000, 200 mM ammonium acetate, 10 mM magnesium acetate, and 20 mM Tris-HCl, pH 7.0, or 200 mM MES, pH 6.5). Rod-shaped crystals of PPARα complexed with compound were obtained within 4−6 days.

Protein Structure Determination and Refinement. Crystals were transferred briefly into a solution of 25% (v/v) glycerol, 26% PEG 4000, 200 mM ammonium acetate, 10 mM magnesium acetate, and 20 mM Tris-HCl, pH 7.0, and flash-cooled in preparation for cryodata collection. Data of PPARα with compound **12** were collected at the Advanced Photon Source, Argonne National Laboratory, on the IMCA-CAT beamline ID-17. Data of PPARα with compound **2** were collected at Brookhaven National Laboratory on the SLS X25 beamline. The images were processed and scaled using HKL2000[22] (Supporting Information). Refinement and model building were carried out using the program MIFit[23] (Supporting Information). The structures have been deposited into the PDB.[11]

In Vitro Assays. A homogeneous, fluorescent polarization PPARα and PPARγ binding assay was used as the primary screen for determining the PPARα and PPARγ binding affinity of compounds.[13] The human functional activity of PPARα and PPARγ agonists was determined by using the GAL4-LBD assays as previously described.[15,17] The in vitro hamster, rat, and mouse PPARα functional activities were tested in the chimeric GAL4/PPARα assay format described for human PPARα as above.[15,17] The data are reported as an EC_{50} value calculated using XLfit 4 parameter fit and floating all parameters.[16] Full length human PPARα and PPARγ co-transfection assays in HepG2 cells were employed for further testing the leading compounds as reported by Mukherjee et al.[12,17]

In Vivo Assays. Human apoA1 Transgenic Mice Lipid Studies. Male 6−8 week old human apoA1 transgenic mice were randomly assigned into different treatment groups and weighed and dosed by oral gavage (5 mL/kg body weight) once a day in the morning with vehicle alone or with compound and allowed free access to food and water. The study duration was 10 days. After dosing on day 10, mice were fasted for 4 h and sacrificed by CO_2 asphyxiation, and blood samples were collected in serum-separating tubes via cardiac puncture for lipid measurements. Livers were dissected out, weighed, and quickly frozen in liquid nitrogen for future RNA analysis. Human apoA1 concentration in serum was measured using the apolipoprotein A1 kit (Polymedco).

Hamsters Lipid Studies. Male Syrian golden hamsters were acclimated to 12 h light/dark reverse light cycle for 7 days with high fat diet, then dosed daily by oral gavage for 21 days while on the same diet. At the end of the experiment, blood samples were drawn retro-orbitally after an 18 h fast and 24 h after the last dose for the determination of serum lipid levels. Livers were dissected out for mRNA analysis.

Statistical Analysis. Mean values for body weight and food consumption, values obtained from clinical laboratory tests, and organ weights of treated groups were compared to those of the control group using Dunnett's test. Statistical comparisons across dose groups were performed using Tukey all pair comparison. A p value of <0.05 was considered as significant changes. Data are expressed as the mean ± SEM.

Acknowledgment. The authors thank Dr. Joel C. Barrish for proofreading the manuscript. The Discovery Toxicology department at Bristol-Myers Squibb is acknowledged for the preclinical safety evaluation of compounds.

Supporting Information Available: Protocols and methods of in vitro and in vivo assays, analytical and spectroscopic data for compounds **12**−**32**, and X-ray crystallographic data of compounds **12** and **2**. This material is available free of charge via the Internet at http://pubs.acs.org.

References

(1) (a) Cannon, C. P.; Braunwald, E.; McCabe, C. H.; Rader, D. J.; Rouleau, J. L.; Belder, R.; Joyal, S. V.; Hill, K. A.; Pfeffer, M. A.; Skene, A. M. Intensive Versus Moderate Lipid Lowering with Statins after Acute Coronary Syndromes. *N. Engl. J. Med.* **2004**, *350*, 1495–1504. (b) LaRosa, J. C.; Grundy, S. M.; Waters, D. D.; Shear, C.; Barter., P.; Fruchart, J. C.; Gotto, A. M.; Greten, H.; Kastelein, J. J.; Shepherd, J.; Wenger, N. K. Intensive Lipid Lowering with Atorvastatin in Patients with Stable Coronary Disease. *N. Engl. J. Med.* **2005**, *352*, 1425–1435. (c) Linsel-Nitschke, P.; Tall, A. R. HDL as a Target in the Treatment of Atherosclerotic Cardiovascular Disease. *Nat. Rev. Drug Discovery* **2005**, *4*, 193–205.

(2) (a) Frick, M. H.; Elo, O.; Haapa, K.; Heinonen, O. P.; Heinsalmi, P.; Helo, P.; Huttunen, J. K.; Kaitaniemi, P.; Koskinen, P.; Manninen, V.; et al. Helsinki Heart Study: Primary-Prevention

Trial with Gemfibrozil in Middle-Aged Men with Dyslipidemia. Safety of Treatment, Changes in Risk Factors, and Incidence of Coronary Heart Disease. *N. Engl. J. Med.* **1987**, *317*, 1237–1245. (b) Rubins, H. B; Robins, S. J.; Collins, D.; Fye, C. L.; Anderson, J. W.; Elam, M. B.; Faas, F. H.; Linares, E.; Schaefer, E. J.; Schectman, G.; Wilt, T. J.; Wittes, J. Gemfibrozil for the Secondary Prevention of Coronary Heart Disease in Men with Low Levels of High-Density Lipoprotein Cholesterol. Veterans Affairs High-Density Lipoprotein Cholesterol Intervention Trial Study Group. *N. Engl. J. Med.* **1999**, *341*, 410–418.

(3) (a) Goldbourt, U.; Yaari, S.; Medalie, J. H. Isolated Low HDL Cholesterol as a Risk Factor for Coronary Heart Disease Mortality. A 21-Year Follow-Up of 8000 Men. *Arterioscler., Thromb., Vasc. Biol.* **1997**, *17*, 107–113. (b) Genest, J. J.; McNamara, J. R.; Salem, D. N.; Schaefer, E. J. Prevalence of Risk Factors in Men with Premature Coronary Artery Disease. *Am. J. Cardiol.* **1991**, *67*, 1185–1189.

(4) (a) Cheng, T. W. P.; Mukherjee, R. PPARs as Targets for Metabolic and Cardiovascular Dieases. *Mini-Rev. Med. Chem.* **2005**, *5*, 741–753. (b) Willson, T. M.; Brown, P. J.; Sternbach, D. D.; Henke, B. R. The PPARs: From Orphan Receptor to Drug Discovery. *J. Med. Chem.* **2000**, *43*, 527–550. (c) Sher, T.; Yi, H. F.; McBride, O. W.; Gonzalez, F. J. cDNA Cloning, Chromosomal Mapping, and Functional Characterization of the Human Peroxisome Proliferator Activated Receptor. *Biochemistry* **1993**, *32*, 5598–5604. (d) Mukherjee, R.; Jow, L.; Noonan, D.; McDonnell, D. P. Human and Rat Peroxisome Proliferator Activated Receptors (PPARs) Demonstrate Similar Tissue Distribution but Different Responsiveness to PPAR Activators. *J. Steroid. Biochem. Mol. Biol.* **1994**, *51*, 157–166.

(5) (a) Staels, B.; Maes, M.; Zambon, A. Fibrates and Future PPARα Agonists in the Treatment of Cardiovascular Diesease. *Nat. Clin. Pract. Cardiovasc. Med.* **2008**, *5*, 542–553. (b) Keating, G. M.; Ormrod, D. Micronised Fenofibrate. *Drugs* **2002**, *62*, 1909–1944.

(6) (a) Athyros, V. G.; Papageorgiou, A. A.; Athyrou, V. V.; Demitriadis, D. S.; Kontopoulos, A. G. Atorvastatin and Micronized Fenofibrate along and in Combination in Type 2 Diabetes with Combined Hyperlipidemia. *Diabetes Care* **2002**, *25*, 1198–1202. (b) Grundy, S. M.; Vega, G. L.; Yuan, Z.; Battisti, W. P; Brady, W. E; Palmisano, J. Effectivenness and Tolerability of Simvastatin Plus Fenofibrate for Combined Hyperlipidemia (SAFARI trial). *Am. J. Cardiol.* **2005**, *95*, 2088–2093.

(7) Trilipix is trademark of Abbott Laboratories, IL.

(8) (a) Grabacka., M.; Plonka., P. M.; Urbanska, K.; Reiss, K. Peroxisome Proliferator-Activated Receptorα Activation Decreases Metastatic Potential of Melanoma Cells in Vitro via Down-Regulation of Akt. *Clin. Cancer Res.* **2006**, *12*, 3028–3036. (b) Pozzi, A.; Ibanez, M. R.; Gatica, A. E.; Yang, S.; Wei, S.; Mei, S.; Falck, J. R.; Capdevila, J. H. Peroxisomal Proliferator-Activated Receptor-α-Dependent Inhibition of Endothelial Cell Proliferation and Tumorigenesis. *J. Biol. Chem.* **2007**, *282*, 17685–17695. (c) Yokoyama, Y.; Xin, B.; Shigeto, T.; Umemoto, M.; Kasai-Sakamoto, A.; Futagami, M.; Tsuchida, S.; Al-Mulla, F.; Mizunuma, H. Clofibric Acid, a Peroxisome Proliferator-Activated Receptor α Ligand, Inhibits Growth of Human Ovarian Cancer. *Mol. Cancer Ther.* **2007**, *6*, 1379–1386. (d) Panigrahy, D.; Kaipainen, A.; Huang, S.; Butterfield, C. E.; Barnes, C. M.; Fannon, M.; Laforme, A. M.; Chaponis, D. M.; Folkman, J.; Kieran, M. W. PPAR.α Agonist Fenofibrate Suppresses Tumor Growth through Direct and Indirect Angiogenesis Inhibition. *Proc. Natl. Acad. Sci. U.S.A.* **2008**, *105* (3), 985–990.

(9) (a) Sierra, M. L.; Beneton, V.; Boullay, A.-B.; Boyer, T.; Brewster, A. G.; Donche, F.; Forest, M.-C.; Fouchet, M.-H.; Gellibert, F. J.; Grillot, D. A.; Lambert, M. H.; Laroze, A.; Le Grumelec, C.; Linget, J. M.; Montana, V. G.; Nguyen, V.-L.; Nicodeme, E.; Patel, V.; Penfornis, A.; Pineau, O.; Pohin, D.; Potvain, F.; Poulain, G.; Ruault, C. B.; Saunders, M.; Toum, J.; Xu, H. E.; Xu, R. X.; Pianetti, P. M. Substituted 2-[(4-Aminomethyl)phenoxy]-2-methylpropionic Acid PPARα Agonists. 1. Discovery of a Novel Series of Potent HDLc Raising Agents. *J. Med. Chem.* **2007**, *50*, 685–695. (b) Brown, P. J.; Winegar, D. A.; Plunket, K. D.; Moore, L. B.; Lewis, M. C.; Wilson, J. G.; Sundseth, S. S.; Koble, C. S.; Wu, Z.; Chapman, J. M.; Lehmann, J. M.; Kliewer, S. A.; Willson, T. M. A Ureido-thioisobutyric Acid (GW9578) Is a Subtype-Selective PPARRα Agonist with Potent Lipid-Lowering Activity. *J. Med. Chem.* **1999**, *42*, 3785–3788. (c) Brown, P. J.; Stuart, L. W.; Hurley, K. P.; Lewis, M. C.; Winegar, D. A.; Wilson, J. G.; Wilkison, W. O.; Ittoop, O. R.; Willson, T. M. Identification of a Subtype Selective Human PPARR Agonist through Parallel-Array Synthesis. *Bioorg. Med. Chem. Lett.* **2001**, *11*, 1225–1227. (d) Miyachi, H.; Nomura, M.; Tanase, T.; Suzuki, M.; Murakami, K.; Awano, K. Enantio-Dependent Binding and Transactivation of Optically Active Phenylpropanoic Acid Derivatives at Human Peroxisome Proliferator-Activated Receptor Alpha. *Bioorg. Med. Chem. Lett.* **2002**, *12*, 333–335. (e) Xu, Y.; Mayhugh, D.; Saeed, A.; Wang, X.; Thompson, R. C.; Dominianni, S. J.; Kauffman, R. F.; Singh, J.; Bean, J. S.; Bensch, W. R.; Barr, R. W.; Osborne, J.; Montrose-Rafizadeh, C.; Zink, R. W.; Yumibe, N. P.; Huang, N.; Luffer-Atlas, D.; Rungta, D.; Maise, D. E.; Mantlo, N. B. Design and Synthesis of a Potent and Selective Triazolone-Based Peroxisome Proliferator-Activated Receptor Agonist. *J. Med. Chem.* **2003**, *46*, 5121–5124. (f) Nomura, M.; Tanase, T.; Ide, T.; Tsunoda, M.; Suzuki, M.; Uchiki, H.; Murakami, K.; Miyachi, H. Design, Synthesis, and Evaluation of Substituted Phenylpropanoic Acid Derivatives as Human Peroxisome Proliferator Activated Receptor Activators. Discovery of Potent and Human Peroxiome Proliferator Activated Rceptor Subtype-Selective Activators. *J. Med. Chem.* **2003**, *46*, 3581–3599. (g) Shi, G. Q.; Dropinski, J. F.; Zhang, Y.; Santini, C.; Sahoo, S. P.; Berger, J. P.; MacNaul, K. L.; Zhou, G.; Agrawal, A.; Alvaro, R.; Cai, T.-Q.; Hernandez, M.; Wright, S. D.; Moller, D. E.; Heck, J. V.; Meinke, P. T. Novel 2,3-Dihydrobenzofuran-2-carboxylic Acids: Highly Potent and Subtype-Selective PPARα Agonists with Potent Hypolipidemic Activity. *J. Med. Chem.* **2005**, *48*, 5589–5599. (h) Yamazaki, Y.; Abe, K.; Toma, T.; Nishikawa, M.; Ozawa, H.; Okuda, A.; Araki, T.; Oda, S.; Inoue, K.; Shibuya, K.; Staels, B.; Fruchart, J. C. *Bioorg. Med. Chem. Lett.* **2007**, *17*, 4689–4693.

(10) Devasthale, P. V.; Chen, S.; Jeon, Y.; Qu, F.; Shao, C.; Wang, W.; Zhang, H.; Cap, M.; Farrelly, D.; Golla, R.; Grover, G.; Harrity, T.; Ma, Z.; Moore, L.; Ren, J.; Seethala, R.; Cheng, L.; Sleph, P.; Sun, W.; Tieman, A.; Wetterau, J. R.; Doweyko, A.; Ghandreasena, G.; Chang, S. Y.; Humphreys, W. G.; Sasseville, V. G.; Biller, S. A.; Ryono, D. E.; Selan, F.; Hariharan, N.; Cheng, R. T. W. Design and Synthesis of *N*-[(4-Methoxyphenoxy)carbonyl]-*N*-[[4-[2-(5-methyl-2-phenyl-4-oxazolyl)ethoxy]phenyl]methyl]glycine [Muraglitazar/BMS-298585], a Novel Peroxisome Proliferator-Activated Receptor α/γ Dual Agonist with Efficacious Glucose and Lipid-Lowering Activities. *J. Med. Chem.* **2005**, *48*, 2248–2250.

(11) PDB deposition number for PPARα and compound **2** is 3KDT. PDB deposition number for PPARα and compound **12** is 3KDU.

(12) Mukherjee, R.; Locke, K. T.; Miao, B.; Meyers, D.; Monshizadegan, H.; Zhang, R.; Search, D.; Grimm, D.; Flynn, M.; O'Malley, K. M.; Zhang, L.; Li, J.; Shi, Y.; Kennedy, L. J.; Blanar, M.; Cheng, P. T.; Tino, J. A.; Srivastava, R. A. Novel Peroxisome Proliferator-Activated Receptor α Agonists Lower Low-density Lipoprotein and Triglycerides, Raise High-density Lipoprotein, and Synergistically Increase Cholesterol Excretion with a Liver X Receptor Agonist. *J. Pharmacol. Exp. Ther.* **2008**, *327*, 716–726.

(13) Seethala, R.; Golla, R.; Ma, Z.; Zhang, H.; O'Malley, K.; Lippy, J.; Cheng, L.; Mookhtiar, K.; Farrelly, D.; Zhang, L.; Hariharan, N.; Cheng., P. T. A Rapid, Homogeneous, Fluorescence Polarization Binding Assay for Peroxisome Proliferator-Activated Receptors Alpha and Gamma Using a Fluorescein-Tagged Dual PPAR Alpha/Gamma Activator. *Anal. Biochem.* **2007**, *363*, 263–274.

(14) Kliewer, S. A.; Sundseth, S. S.; Jones, S. A.; Brown, P. J.; Wisely, G. B.; Koble, C. S.; Devchand, P.; Wahli, W.; Willson, T. M.; Lenhard, J. M.; Lehmann, J. M. Fatty Acids and Eicosanoids Regulate Gene Expression through Direct Interactions with Peroxisome Proliferator-Activated Receptors Alpha and Gamma. *Proc. Natl. Acad. Sci. U.S.A.* **1997**, *94*, 4318–4323.

(15) Mukherjee, R. PPARs: Versatile Targets for Future Therapy for Obesity, Diabetes and Cardiovascular Diseases. *Drug News Perspect.* **2002**, *15*, 261–267.

(16) Osumi, T.; Wen, J. K; Hashimoto, T. Two Cis-Acting Regulatory Sequences in the Peroxisome Proliferator-Pesponsive Enhancer Region of Rat Acyl-CoA Oxidase Gene. *Biochem. Biophys. Res. Commun.* **1991**, *175*, 866–871.

(17) Mukherjee, R.; Sun, S; Santomenna, L.; Miao, B.; Walton, H.; Liao, B.; Locke, K.; Zhang, J. H.; Nguyen, S. H.; Zhang, L. T.; Murphy, K.; Ross, H. O.; Xia, M. X.; Teleha, C.; Chen, S. Y.; Selling, B.; Wynn, R.; Burn, T.; Young, P. R. Ligand and Coactivator Recruitment Preferences of Peroxisome Proliferator Activated Receptor Alpha. *J. Steroid Biochem. Mol. Biol.* **2002**, *81*, 217–225.

(18) (a) Berthou, L.; Duverger, N.; Emmanuel., F.; Langouët, S.; Auwerx, J.; Guillouzo, A.; Fruchart, J. C.; Rubin, E.; Denèfle, P.; Staels, B.; Branellec, D. Opposite Regulation of Human versus Mouse Apolipoprotein A-I by Fibrates in Human Apolipoprotein A-I Transgenic Mice. *J. Clin. Invest.* **1996**, *97*, 2408–2416. (b) Rubin, E. M.; Ishida, B. Y.; Clift, S. M.; Krauss., R. M. Expression of Human Apolipoprotein A-I in Transgenic Mice Results in Reduced Plasma Levels of Murine Apolipoprotein A-I and the Appearance of Two New High Density Lipoprotein Size Subclasses. *Proc. Natl. Acad. Sci. U.S.A.* **1991**, *88*, 434–438.

(19) Wang, P. R.; Guo, Q.; Ippolito, M.; Wu, M.; Milot, D.; Ventre, J.; Doebber, T.; Wright, S. D.; Chao, Y. S. High Fat Fed Hamster, a Unique Animal Model for Treatment of Diabetic Dyslipidemia

with Peroxisome Proliferator Activated Receptor Alpha Selective Agonists. *Eur. J. Pharmacol.* **2001**, *427*, 285–293.
(20) (a) Spady, D. K.; Dietschy, J. M. Sterol Synthesis in Vivo in 18 Tissues of the Squirrel Monkey, Guinea Pig, Rabbit, Hamster, and Rat. *J. Lipid Res.* **1988**, *24*, 303–315. (b) Nistor, A.; Bulla, A.; Filip, D. A.; Radu, A. The Hyperlipidemic Hamster as a Model of Experimental Atherosclerosis. *Atherosclerosis* **1987**, *68*, 159–173.
(21) Cronet, P.; Petersen, J.; Folmer, R.; Blomberg, N.; Sjöblom, K.; Karlsson, U.; Lindstedt, E.-L.; Bamberg, K. Structure of the PPARα and -γ Ligand Binding Domain in Complex with AZ 242; Ligand Selectivity and Agonist Activation in the PPAR Family. *Structure* **2001**, *9*, 699–706.
(22) Otwinowski, Z.; Minor, W. Processing of X-Ray Diffraction Data Collected in Oscillation Mode. In *Methods in Enzymology, Macromolecular Crystallography, Part A*; Carter, C. W., Jr., Sweet, R. M., Eds.; Academic Press: New York, 1997; Vol. 276, pp 307−326.
(23) *MIFit Software. Consortium Version for Windows*, version 7.1.rc1; Rigaku Americas Corporation: The Woodlands, TX, 2003−2007.